SARS-CoV-2 differs from SARS-CoV in the requirements for receptor expression and proteolytic activation to trigger cell-cell fusion and is not inhibited by Bromhexine

Bojan F. Hörnich[1], Anna K. Großkopf[1], Sarah Schlagowski[1], Matthias Tenbusch[2], Frank Neipel[2], Alexander S. Hahn[1]

[1]Nachwuchsgruppe Herpesviren, Abteilung Infektionsbiologie, Deutsches Primatenzentrum – Leibniz-Institut für Primatenforschung, Göttingen, Germany
[2]Virologisches Institut, Universitätsklinikum Erlangen, Erlangen, Germany

Correspondence to: ahahn@dpz.eu

ABSTRACT
The SARS-Coronavirus-2 (SARS-CoV-2) infects cells through interaction of its spike protein (SARS-CoV-2-S) with the ACE2 receptor and activation by proteases, in particular TMPRSS2. Viruses can also spread through fusion of infected with uninfected cells. We therefore analyzed cell-cell fusion activity of SARS-CoV-2-S with regard to the requirements for ACE2 expression, proteolytic activation, and sensitivity to inhibitors and compared it to SARS-CoV-S. We compared S-protein-driven fusion with target cells recombinantly overexpressing ACE2, TMPRSS2, or both. SARS-CoV-2-S-driven fusion was moderately increased by TMPRSS2 and strongly by ACE2, while the reverse observation was made for SARS-CoV-S. TMPRSS2-mediated effects were inhibited by the serine protease inhibitor Camostat. Effector-target-cell fusion by SARS-CoV-2-S was only affected by Camostat when receptor expression was limiting or when the S1/S2 cleavage site was mutated. Mutational ablation of the SARS-CoV-2-S S2' cleavage site abrogated any effects of TMPRSS2 on fusion. Mutation of the SARS-CoV-2-S S1/S2 cleavage site reduced effector-target-cell fusion when ACE2 or TMPRSS2 were limiting. When both factors were abundant, initial target-effector-cell fusion was unaltered, but syncytia remained smaller over time. Overall, its polybasic cleavage site renders SARS-CoV-2-S-mediated cell-cell fusion less dependent on TMPRSS2 activity on target cells. Unexpectedly, we observed enhancement of SARS-CoV-2-S-mediated fusion by Bromhexine, another TMPRSS2 inhibitor. This effect required intact proteolytic cleavage sites, suggesting interference of Bromhexine with proteolytic priming, but not in a therapeutically desired way. Infection with SARS-CoV-2-S-pseudotyped particles clearly differed in the requirements for proteolytic activation from cell-cell fusion. TMPRSS2 strongly enhanced infection, which was reversed by Camostat but not by Bromhexine.

IMPORTANCE
Cell-cell fusion allows the virus to infect additional target cells without the need to produce free virus. Fusion likely also contributes to tissue damage by creating virus-infected syncytia. Our results demonstrate that the S2' cleavage site is essential for activation by TMPRSS2 in trans and unravel important differences between SARS-CoV and SARS-CoV-2. Bromhexine, an inhibitor of the TMPRSS2 protease, is currently tested in clinical trials against COVID-19. Our results indicate that Bromhexine does not inhibit SARS-CoV-2-S-mediated particle entry and enhances fusion. We therefore caution against overly optimistic use of Bromhexine in higher dosage in clinical trials or as a therapy, at least until its effects on SARS-CoV-2 spike activation are better understood. The related compound Ambroxol, which similar to Bromhexine is clinically used as an expectorant, did not exhibit activating effects on SARS-

CoV-2 S-mediated fusion and may therefore currently represent a better choice in therapeutic regimens for COVID-19.

INTRODUCTION

The COVID-19 disease spectrum is caused by the severe acute respiratory syndrome-related coronavirus 2 (SARS-CoV-2), which was first identified in patients with pneumonia of unknown origin in the city of Wuhan, China (1). While first characterized as a pneumonia, COVID-19 probably affects a number of organ systems (2–4). SARS-CoV-2 was shown to use the ACE2 receptor, which was previously described as receptor for the closely related SARS-CoV (5), for the infection of human cells (1, 6, 7). For the proteolytic activation of the viral spike protein, a prerequisite for fusion activity of coronaviruses (reviewed in (8)), the type-II transmembrane serine protease TMPRSS2 (7, 9) as well as the related TMPRSS4 (2) were reported to be of critical importance. In addition, TMPRSS2 was demonstrated to colocalize with the ACE2 receptor (10), and therefore may be biologically particularly relevant. Depending on the cell type, SARS-CoV-2 spike-driven entry can also occur through endocytotic pathways where virus-cell fusion is most likely activated by cathepsins (7). Another study reported that several members of the TMPRSS family can activate SARS-CoV-2 spike-mediated membrane fusion (11). The proposed mechanisms for spike priming and initiation of fusion therefore require further clarification.

It was recently discovered that the polybasic S1/S2 cleavage site of SARS-CoV-2 is required for efficient infection of lung-derived cells (12) and promotes the formation of syncytia. Understanding syncytium formation may be important as large syncytial elements are reported to constitute a hallmark of COVID-19-associated pathology (13). Nevertheless, the exact contribution of the two known proteolytic priming sites to cell-cell fusion and their protease usage are not entirely clear. To address these questions, we mutated the S1/S2 site as well as the S2' site, we interrogated the effects of proteolytic activation by using inhibitors of TMPRSS2, and we analyzed the effects of different levels of protease and receptor expression on fusion activity.

TMPRSS2, which is expressed in airway cells (14), may be amenable to specific inhibition by Bromhexine (15), a molecule normally used as an expectorant that thins phlegm and eases coughing and widely known as a popular over-the-counter medication, which would make its repurposing for COVID-19 particularly attractive. For these or additional reasons, Bromhexine is now being tested in at least three clinical trials for efficacy against COVID-19 (NCT04355026, NCT04273763, NCT04340349). We therefore tested the effect of the specific TMPRSS2 inhibitor Bromhexine on spike protein-mediated cell-cell fusion and SARS-CoV-2-S driven cell entry and compared its potency to the serine protease inhibitor Camostat.

RESULTS

We chose 293T cells as effector cells, e.g. the cell expressing the viral glycoproteins, for i) their high transfection efficiency and protein expression and ii) their ability to be lifted without trypsinization. We resorted to a system that is also used for two-hybrid screenings, using a VP16-Gal4 transcription factor in one cell and a Gal4-response element-driven reporter construct in the other cell, which results in strong transactivation and reporter gene expression after cell-cell fusion.

<u>SARS-CoV-2 spike protein mediates robust fusion of 293T cells transfected with ACE2 and TMPRSS2 and the S2' proteolytic priming site is critical for fusion activity.</u>

We transfected 293T target cells with ACE2 and TMPRSS2 expression plasmids and Gal4 response element driven TurboGFP-luciferase reporter plasmid (Gal4-TurboGFP-Luc) and effector cells with codon-optimized SARS-CoV-2-S or SARS-CoV-S expression plasmid, as well as with a plasmid encoding the Gal4 DNA binding domain fused to the VP16 transactivator. In addition, we tested SARS-CoV-2-S_S2'mut, in which the two basic residues of the S2' priming site have been replaced with two alanine residues, and SARS-CoV-2-S_S1/S2mut, in which the polybasic furin recognition sequence has been replaced with four alanine residues, as fusion effectors (Fig. 1 A, schematic drawn after (16)). We observed robust fusion with SARS-CoV-2-S, practically unaltered or even increased fusion activity with SARS-CoV-2-S_S1/S2mut, and drastically reduced fusion activity with SARS-CoV-2-S_S2'mut (Fig. 1 B). Expression of the individual proteins was verified by Western blot analysis (Fig. 1 C). Apparent expression levels of SARS-CoV-S as assayed by Western blot were seemingly lower, but this may be owed to different glycosylation, proteolytic cleavage and transfer or detection and was not reflected in the fusion activity. Clearly detectable bands of lower molecular weight, indicative of proteolytic processing, were only observed with SARS-CoV-2 wt spike. The fusion activity as observed by measuring luciferase activity was also reflected in the formation of TurboGFP-luciferase expressing syncytia as observed under the microscope (Fig. 1 D). As we cocultured the cells for 48h, formation of relatively large syncytia was observable with SARS-CoV-2-S and SARS-CoV-S, and these are most likely not only formed by the initial fusion event between effector and target cells, but then grow in size through fusion with neighboring cells. Interestingly, while the overall measured reporter activity was even slightly increased with the SARS-CoV-2 S1/S2 mutant in the presence of TMPRSS2 and ACE2, corresponding to visibly more numerous syncytia, these syncytia appeared to be smaller in size. To limit the effect of syncytia extension over time and potential cytotoxic effects of such extended syncytia formation, we decided to measure reporter activity after 24h instead of 48h for the following experiments.

<u>SARS-CoV-2-S-mediated cell-cell fusion is dependent on ACE2 receptor expression and is less restricted by proteolytic activation in trans than SARS-CoV-S-mediated fusion.</u>

For a comprehensive analysis, we measured fusion with target cells that were co-transfected with ACE2 and TMPRSS2 expression plasmids, and in addition to cells transfected with either ACE2 or TMPRSS2 expression plasmid alone. As fusion effectors, SARS-CoV-S, SARS-CoV-2-S as well as SARS-CoV-2_S1/S2mut and SARS-CoV-2_S2'mut were included. To test the effects of TMPRSS2 inhibition by small molecules on the activation of wt SARS-CoV-2-S and the two mutants as well as SARS-CoV-S, we incubated the different target cells with Bromhexine, a specific inhibitor of TMPRSS2 (15), the chemically related compound Ambroxol, or Camostat, an irreversible inhibitor of TMPRSS2 and many serine proteases in general (17, 18), at 50 µM (Fig. 2 A). We chose this high concentration, which is most likely outside of any therapeutic range, as overexpression of TMPRSS2 may shift the EC50 considerably upwards.

As observed before (Fig. 1 B), in the presence of ACE2 and TMPRSS2, both SARS-CoV-S and SARS-CoV-2-S exhibited strong fusion activity, as did the SARS-CoV-S-S1/S2mut protein. SARS-CoV-S-S2'mut on the other hand was strongly impaired under these conditions.

ACE2 expression alone was sufficient for induction of high fusion activity of SARS-CoV-2-S but induced only moderate activity of SARS-CoV-S. Levels of ACE2 expression were higher in single-transfected cells (Fig. 2 C). This observation is compatible with data from the literature stating that ACE2 is cleaved by TMPRSS2 (10), which conceivably reduces detection by Western blot, in addition to potential competition effects between expression plasmids.

Nevertheless, SARS-CoV-2-S-driven fusion was clearly not limited by TMPRSS2 expression, and reached highest activity when only ACE2 was expressed. The S1/S2 cleavage site mutant of SARS-CoV-2 on the other hand exhibited reduced activation in the presence of ACE2 without additional TMPRSS2 activity, whereas the S2' mutant exhibited impaired but detectable fusion activity when ACE2 was overexpressed. Overexpression of TMPRSS2 did not increase fusion acitivity of the S2' mutant spike. Conversely, SARS-CoV-S-driven fusion was clearly more enhanced by overexpression of TMPRSS2 than by overexpression of ACE2, reaching highest activity under conditions where only TMPRSS2 was recombinantly expressed, and was only weakly activated by ACE2 expression in the absence of recombinant TMPRSS2 expression (Fig. 2 A and B).
We observed that cell-cell fusion by SARS-CoV-S and SARS-CoV2-S was not inhibited by Bromhexine, and only SARS-CoV-S activity was slightly inhibited by Ambroxol in the presence of TMPRSS2. Surprisingly, we observed an induction of SARS-CoV2-S fusion activity in the presence of Bromhexine, significantly so when ACE2 and TMPRSS2 were coexpressed. Similarly, Camostat did not reduce SARS-CoV-2-S-mediated fusion in this setting unless TMPRSS2 was overexpressed without ACE2. However, both SARS-CoV-2-S1/S2mut and even more pronouncedly SARS-CoV-S exhibited a significantly reduced fusion activity in the presence of Camostat. The strong induction of SARS-CoV-S-mediated fusion by TMPRSS2 was clearly reversed by Camostat but not by Bromhexine. Notably, Camostat did not exert any inhibitory effect on the remaining fusion activity of the SARS-CoV-2-S2'mut mutant, nor did TMPRSS2 expression induce activity of this mutant, compatible with the S2' site being the primary target of TMPRSS2 in trans.
Taken together, we observed robust SARS-CoV-2 spike protein-mediated cell-cell fusion that was not dependent on exogenous TMPRSS2 expression and that was not inhibited by Bromhexine. Instead, fusion was enhanced by Bromhexine. Cell-cell fusion mediated by SARS-CoV-2-S was clearly not at all or to a much lesser degree restricted by serine protease activity on target cells than fusion by SARS-CoV-S.

Bromhexine enhances SARS-CoV-2-S-mediated fusion in the presence of TMPRSS2.
To further explore the paradoxical effect of the putative TMPRSS2 inhibitor Bromhexine on fusion activity, we performed fusion reactions in the presence of Bromhexine and Ambroxol at different concentrations (Fig. 3). In order to eliminate potential systematic errors, we deviated from our previous protocol, cocultured for 48h instead of 24h, and cotransfected the reporter plasmid into the effector instead of the target cells, this time using a different luciferase reporter without TurboGFP. We again did not observe inhibition by Bromhexine, but a dose-dependent enhancement. Ambroxol treatment on the other hand did not lead to a similar enhancement, but possibly to a slight decrease in activity at 50µM. As a control fusion protein that works with practically any cell type, we included VSV-G. While VSV-G is physiologically pH-activated for full fusion activity (19), it reportedly exhibits considerable activity without pH priming (20, 21). VSV-G-mediated fusion activity was not increased by Bromhexine.

Entry of SARS-CoV-2-S-pseudotyped lentiviruses is dependent on TMPRSS2 and is not inhibited by Bromhexine irrespective of the presence of TMPRSS2.
To compare our findings on cell-cell fusion to spike protein-driven entry, we used lentiviral particles expressing GFP as reporter gene, pseudotyped with SARS-CoV-2-S. We found that TMPRSS2 expression was clearly required for efficient infection of 293T cells by SARS-CoV-2-S-pseudotyped particles (Fig. 4 A). ACE2 overexpression alone also enhanced infection, but

considerably less efficiently and barely above the detection limit, which may be owed to our lentiviral system. The TMPRSS2-mediated enhancement was clearly reversed by addition of Camostat, but not by addition of Bromhexine or Ambroxol. Infection with a VSV-G pseudotyped lentivirus was not affected appreciably by expression of ACE2 and/or TMPRSS2. Bromhexine exhibited a slightly inhibitory effect on VSV-G driven infection at 50 µM, whereas Ambroxol did not, possibly hinting at some effect of Bromhexine on endocytotic processes. These observations were again corroborated by fluorescence microscopy (Fig. 4 C).

DISCUSSION

We have established a two-hybrid-based protocol for measuring SARS-CoV-spike-mediated cell-cell fusion that allows for the quantitation of cell-cell fusion by luciferase activity and visualization of syncytia by GFP fluorescence. Our findings that SARS-CoV and SARS-CoV-2 spike protein-mediated fusion activity is activated by the ACE2 receptor is in accordance with published data (11), whereas our finding that SARS-CoV-2-S-mediated fusion depends relatively more on receptor expression and less on proteolytic activation than SARS-CoV-S-mediated fusion is novel. Further, we have established the S2' site of SARS-CoV-2-S as the target for TMPRSS2-mediated activation.

In our system, TMPRSS2 co-expression on ACE2 expressing target cells was not required for SARS-CoV-2-S-mediated fusion of 293T cells comparable with results of Ou et al. where ACE2 expression alone was also sufficient to induce cell-cell fusion without addition of exogenous protease (11). Furthermore, we did not observe any effect on SARS-CoV-2-S-mediated fusion activity upon inhibition of TMPRSS2 on target cells by the serine protease inhibitor Camostat. Together, these results imply that proteolytic activity may not be a limiting factor for cell-cell fusion in 293T cells. This is also in accordance with another report, which demonstrates that several other proteases from the TMPRSS family can activate SARS-CoV-2 spike protein for fusion (11). A recent preprint demonstrated that upon cotransfection of spike, ACE2, and TMPRSS2, TMPRSS2 accelerates fusion. The size of the resulting syncytia only showed a TMPRSS2 dependency within the first 12h but was independent after 24h (22), which is compatible with our observations at this timepoint. It should be noted that SARS-CoV-2 was activated moderately by TMPRSS2 expression in our experimental setting when ACE2 was limiting. Thus, it seems as if full proteolytic activation may overcome low receptor levels, while high receptor levels can compensate for incomplete proteolytic activation.

While SARS-CoV-S-mediated cell-cell fusion was also activated by ACE2 alone, activation was much higher in the presence of TMPRSS2, indicating stronger dependence of SARS-CoV-S on TMPRSS2, compatible with the monobasic S1/S2 cleavage site in the SARS-CoV spike protein. In line with this observation, SARS-CoV-S-mediated cell-cell fusion was clearly sensitive to Camostat, suggesting that a serine protease activates the SARS-CoV spike on target cells. Interestingly, mutational ablation of the S1/S2 cleavage site of SARS-CoV-2-S rendered the mutated spike protein sensitive to inhibition by Camostat, confirming that TMPRSS2 or a related protease is needed for processing at the S2' site. In addition, in the absence of TMPRSS2, SARS-CoV-2-S_S1/S2mut was clearly impaired with regard to fusion activity (Fig. 2 A). Conversely, mutation of the S2' priming site abrogated any effects of TMPRSS2 on SARS-CoV-2-mediated fusion, e.g. when TMPRSS2 alone was provided by means of recombinant expression (Fig. 2 A), confirming this site as the primary target of TMPRSS2 for fusion activation.

It remains to be determined how processing at the S1/S2 site renders SARS-CoV-2-S-mediated cell-cell fusion at least partially independent of processing by TMPRSS2 at the S2' site. It is tempting to speculate that a broader range of proteases can attack the S2' site after it has been liberated. Our results with the S2' mutant, which exhibited impaired fusion activity, clearly demonstrate that cleavage at the S1/S2 site alone is not sufficient for full fusion activity and likely requires additional processing at S2'.

Another unexpected observation was that both the S2' and S1/S2 mutants exhibited reduced processing, as observed in Figs. 1 C and 2 C. This may hint at a more complicated processing pattern than just furin cleavage, possibly also involving the S2' site. We therefore speculate that processing by TMPRSS2 or similar proteases may also occur in cis. This notion would be compatible with observations in a recent report, where in cis activation by TMPRSS2 can overcome inhibitory effects on fusion by IFITM proteins expressed in cis (22). A more trivial explanation could be that the S2' mutant differs slightly with regard to blotting efficiency or detection limit in Western blot analysis.

As SARS-CoV-2-S did not require TMPRSS2 on target cells for robust cell-cell fusion, our attempts to test the impact of Bromhexine as a specific inhibitor of TMPRSS2 on SARS-CoV-2-S-mediated fusion activity were somewhat artificial. Nevertheless, SARS-CoV-S-mediated fusion was clearly enhanced by TMPRSS2, as was fusion by the SARS-CoV-2-S_S1S1' mutant, and both were inhibited by Camostat but not by Bromhexine. Therefore, our finding that Bromhexine specifically enhanced fusion of 293T cells in the presence of SARS-CoV-2-S, ACE2, and TMPRSS2 is something that we cannot explain easily. According to our results the Bromhexine-mediated enhancement was specific for SARS-CoV-2 spike protein and was not seen with VSV-G as fusion effector, nor did we observe significant effects with the SARS-CoV-2-S mutants and SARS-CoV-S (Figs. 2 A). We observed some inhibition of SARS-CoV-S-mediated fusion in the presence of 50µM Ambroxol, which may hint at some activity of this substance against TMPRSS2. The observation that the paradoxical effect of Bromhexine was reduced or abrogated by mutation of the proteolytic priming sites strongly suggests that Bromhexine somehow modulates proteolytic processing. It is at the moment not clear by what mechanism of action Bromhexine modulates TMPRSS2 activity, and we therefore cannot exclude that processing of some substrates is actually enhanced or altered instead of inhibited, as reported for several substrates (15, 23). Activity of Bromhexine against TMPRSS2-mediated receptor shedding, but lower or no activity against spike processing could also explain our observations. Inhibition of ACE2 shedding would also be compatible with the slight increase in fusion activity that we observed with SARS-CoV-2-S in the presence of Camostat when ACE2 and TMPRSS2 were coexpressed (Fig. 2 A). Another explanation would be that unknown endogenous protease(s) process SARS-CoV-2-S in a manner that is more favorable for cell-cell fusion than processing by TMPRSS2, and that these proteases compete for the spike protein. Given that in enteric organoids, SARS-CoV-2 is primarily activated by TMPRSS4 (2), and probably cooperatively with TMPRSS2, competition between proteases could conceivably occur.

Compared to another study (24), our fusion assay yields slightly different results, with SARS-CoV-2-S-mediated fusion appearing less dependent on activation by TMPRSS2. This could be due to differences in the protocol. The study by Yamamoto et al. allowed only for very short contact times of 4h and used non-adherent 293T FT cells, whereas we cocultured the cells for a longer time, which allows for extended contact between cells and may enable the action of different proteases. Our finding that TMPRSS2 is not required for fusion is in line with a recent report making the same observation (25). In general, we observed a higher fusion activity with our SARS-CoV-2 S1/S2 spike mutant than was observed with furin

cleavage site mutants in previous studies (12, 26), but only when TMPRSS2 was recombinantly overexpressed together with ACE2. When only ACE2 or only TMPRSS2 were recombinantly expressed, SARS-CoV-2_S1/S2_mut fusion activity was strongly impaired (Fig. 2 A). It should also be noted, that we left the loop intact and only replaced the basic residues with alanine in our mutant whereas other groups deleted the loop structure. Nevertheless, our approach clearly rendered the spike protein more dependent on serine protease activity, likely towards the S2' site, as SARS-CoV-2_S1/S2mut fusion activity was significantly inhibited by Camostat (Fig. 2 A). Taken together, our results actually reconcile several seemingly conflicting observations by other groups. The strong reduction in fusion activity by mutation of the S1/S2 site observed in one study in Vero (12) is reflected in our experimental conditions with only TMPRSS2 and endogenous levels of ACE2 expression, whereas our findings of more or less normal fusion activity under conditions of high-level ACE2 and TMPRSS2 expression are similar to the findings of another group with ACE2 overexpressing cells and addition of Trypsin or HAT (26).

Overall, we propose that the dependence on S1/S2 cleavage, activity of TMPRSS2 or a related protease and receptor expression are interdependent, where one factor can to a large degree compensate for another, e.g. more extensive proteolytic activation can render the spike more fusogenic even with lower receptor levels. Similarly, whether and to what extent furin cleavage or processing by additional proteases (27) occur may depend on the levels of furin expression on producer cells relative to the synthesis rate of the spike protein. Pre-processed spike protein may then be less dependent on proteolytic activation in trans or can fuse more easily at lower receptor levels.

In a lentiviral pseudotype system, our results were clear: Bromhexine or the related compound Ambroxol did not specifically modulate infection of 293T cells transfected with expression plasmids for ACE2 and TMPRSS2. Infection of 293T was clearly enhanced by overexpression of TMPRSS2, and this enhancement was not reversed by Bromhexine but it was reversed by addition of Camostat.

According to our results the requirements for cell-cell fusion and virus-cell fusion differ: Additional TMPRSS2 activity drastically enhanced pseudotype entry into transfected 293T but was not needed for cell-cell fusion with identically transfected 293T cells. Similar observations were previously made for SARS-CoV (28). The interpretation of these results is complicated by the ability of virus particles to enter cells through both direct membrane fusion or through an endocytotic pathway, and by different pre-priming states of viral spike proteins depending on proteolytic activity in the producer cell (29). As activation of the spike protein is expected to differ between organ systems depending on the presence of different proteolytic activities, these processes ultimately need to be studied in appropriate tissue systems or animal models. It is tempting to speculate that the relative to SARS-CoV more relaxed requirements for cell-cell fusion with regard to proteolytic activation contribute to the broad organ tropism and neuroinvasion by SARS-CoV-2, as well as the clinically observed formation of extended syncytia (13). Irrespective of the role of cell-cell fusion in COVID-19, in light of the observed paradoxical activation of cell-cell fusion by Bromhexine and its lack of inhibitory activity against entry of SARS-CoV-2 spike-pseudotyped lentiviruses on TMPRSS2 expressing cells, we would at the moment caution against clinical use of Bromhexine for treatment or prophylaxis of COVID-19.

MATERIAL AND METHODS

Cell Culture

All cell lines in this study were incubated at 37°C and 5% CO_2. 293T (a kind gift from Vladan Rankovic and originally purchased from the ATCC, Göttingen) were cultured in Dulbecco's Modified Eagle Medium (DMEM), high glucose, GlutaMAX, 25mM HEPES (Thermo Fisher Scientific) supplemented with 10% fetal calf serum (FCS) (Thermo Fisher Scientific), and 50µg/ml gentamycin (PAN Biotech). For seeding and sub-culturing of cells the medium was removed, the cells were washed with PBS (PAN-Biotech) and detached with Trypsin (PAN-Biotech). All transfections were performed using PEI (Polysciences) in a 1:3 Ratio (µg DNA/µg PEI) mixed in OptiMEM.

Plasmids

Expression plasmids for pQCXIPBL-hTMPRSS2 (30), pCG1-SARS-2-S_humanized (31), and pCG1-SARS S (32) are described elsewhere. For generation of pVAX1-SARS2-S the codon-optimized sequence encoding the spike protein of SARS-CoV-2 was amplified by PCR and cloned into the pVAX1 backbone. psPAX2 and pMD2.G were a gift from Didier Trono (Addgene plasmid # 12260, Addgene plasmid # 12259) and pLenti CMV GFP Neo (657-2) was a gift from Eric Campeau & Paul Kaufman (Addgene plasmid # 17447). Expression plasmids SARS-Cov-2-S_S2'mut and SARS2-S_S1/S2mut were generated from pCG1_SL-Cov_Wuhan-S_humanized SARS-S by PCR based using around-the-horn PCR mutagenesis using Phusion PCR, T4 PNK and Quick ligase (all from New England Biolabs) mutation of the SARS2-S S1S2 and the S2' cleavage site to alanine using the following primers: primers S1-S2 AAAA mut for V2 (CTGCCTCTGTGGCCAGCCAGAGCATC), S1-S2 AAAA mut rev V2 (CAGCGGCGGGGCTGTTTGTCTGTGTCTG), S2 to AA mut_Foward (GCCAGCTTCATCGAGGACCTGCTG) and S2 to AA mut_Reverse (AGCGCTGGGCTTGCTAGGATCGG). Sequence integrity was verified by sequencing of the coding region. Plasmid pCG1-SARS-Cov-2-S_S2'mut contains a silent G to T mutation in the codon for leucine 441.

The Gal4-Luc reporter plasmid encoding firefly luciferase under the control of an activator sequence that binds the Gal4 transcription factor has been described elsewhere (28). The Gal4 DNA binding domain VP16 fusion plasmid corresponds to Genbank identifier X85976. The TurboGFP-Luciferase fusion reporter gene was constructed using Gibson Assembly Master Mix (New England Biolabs) to insert the TurboGFP open reading frame with a Ser-Gly-Ser-Gly Linker in front of the Met codon of the luciferase open reading frame. Before assembly, the two fragments were generated using Phusion PCR (New England Biolabs) by amplifying the TurboGFP open reading frame from the vector pGIPZ (Thermo Scientific Open Biosystems) using the primers TurboGFP for Gal4Luc before ATG ov (GGTACTGTTGGTAAAATGGAGAGCGACGAGAGC) and TurboGFP rev (TTCTTCACCGGCATCTGCATC), and the Gal4-Luc backbone by amplification with primer Gal4Luc before ATG rev (TTTACCAACAGTACCGGAATGC) and primer Luc for SGSG TurboGFP overhang (GATGCAGATGCCGGTGAAGAAAGCGGTAGCGGTATGGAAGACGCCAAAAACATAAAG).

Western Blot

Protein expression was analyzed by polyacrylamide gel electrophoresis on 8%-16% gradient precast gradient gels (Thermo) and Western blotting using antibodies to ACE2 (AF933, R&D Systems), c-Myc-epitope (clone 9E10, Santa Cruz Biotechnology), SARS-Spike (NB100-56578, Novus Biologicals) and GAPDH (GenScript) in NETT-G (150 mM NaCl, 5mM EDTA, 50 mM Tris, 0.05% Triton X-100, 0.25% gelatin, pH 7.5) and donkey anti-mouse horseradish peroxidase (HRP)-coupled (Dianova), goat anti-rabbit HRP-coupled (Life Technologies) or rabbit anti-

goat HRP-coupled (Proteintech) secondary antibody in 5% dry milk powder in PBS with 0.05% Tween 20. Imaging was performed using Immobilon Forte substrate (Merck) on an INTAS ECL ChemoCam system.

Fusion-Assay

293T target-cells were seeded in a 48-well plate at 50.000 cells/well and transfected with Vp16-Gal4 (Fig. 3) or Gal4-TurboGFP-Luciferase expression plasmid (Gal4-TurboGFP-Luc, Figs. 1 and 2) as well as expression plasmids for ACE2 and TMPRSS2 as indicated. In case only ACE2 or TMPRSS2 were transfected the missing amount of DNA was replaced by empty vector. 293T effector-cells were seeded in a 10 cm dish at 70-80% confluency and transfected with either the Vp16-Gal4 (Figs. 1 and 2) or Gal4-Luciferase (Fig. 3) expression plasmid as well as expression plasmids for SARS-CoV-2-S, SARS-CoV-2-S_S2'mut, SARS-Cov-2-S_S1/S2mut SARS-CoV-S, VSV-G glycoproteins or pcDNA6/V5-HisA (Thermo). 24h after transfection, target-cells were pre-incubated with Bromhexine hydrochloride (Merck), Ambroxol hydrochloride (Merck) or Camostat mesylate (Tocris) for 30 min at twice the indicated concentration. Effector-cells were then added to the target-cells in a 1:1 ratio reaching the final inhibitor concentration. After 24-48h GFP-fluorescence was detected using a Vert.A1 Fluorescence Microscope and ZEN-Software (Zeiss), luciferase activity was analyzed using the PromoKine Firefly luciferase Kit or Beetle-Juice Luciferase Assay according to manufacturer's instructions and a Biotek Synergy 2 platereader. Statistical analysis was performed using GraphPad Prism 6.

Production of lentiviral and pseudoparticles and transduction experiments

Lentiviral pseudoparticles were produced by transfecting 293T cells with expression plasmids for psPAX2, pLenti-CMV-GFP and either SARS2-Spike (pVAX1-SARS2-S) or VSV-G. The cell culture supernatants were harvested three days post transfection followed by addition of fresh media and again six days post transfection. The supernatants were passed through a 0.45µm CE-Filter, and the SARS-Cov-2-S pseudoparticles were concentrated via low speed centrifugation at 4°C for 16h at 4200xg. The SARS spike and VSV-G lentiviral pseudoparticles were used to transduce 293T transfected with TMPRSS2 and ACE2 expression plasmids. 48 h after transfection with control or ACE2 and TMPRSS2 expression plasmids, the pseudoparticles were added to the cells. Cells transduced with pseudoparticles were harvested 48 h after transduction using trypsin. Trypsin activity was inhibited by adding 5% FCS in PBS, and after washing with PBS the cells were fixed with 4% formaldehyde (Roth) in PBS. The percentages of GFP-positive cells were determined using a LSRII flow cytometer, and at least 10000 cells were analyzed. Flow cytometry data was processed using Flowing Software and statistical analysis was performed using GraphPad Prism 6.

ACKNOWLEDGEMENTS

We thank Stefan Pöhlmann and Markus Hofmann for sharing reagents and for critical reading of the manuscript and helpful discussions. We also thank Armin Ensser and Florian Full for helpful discussions.

FUNDING

This work was supported by grant HA 6013/4-1 to A.S.H. from the Deutsche Forschungsgemeinschaft and by grant 2019.027.1 to A.S.H. from the Wilhelm-Sander-Stiftung.

REFERENCES

1. Zhou P, Yang X-L, Wang X-G, Hu B, Zhang L, Zhang W, Si H-R, Zhu Y, Li B, Huang C-L, Chen H-D, Chen J, Luo Y, Guo H, Jiang R-D, Liu M-Q, Chen Y, Shen X-R, Wang X, Zheng X-S, Zhao K, Chen Q-J, Deng F, Liu L-L, Yan B, Zhan F-X, Wang Y-Y, Xiao G-F, Shi Z-L. 2020. A pneumonia outbreak associated with a new coronavirus of probable bat origin. Nature 579:270–273.
2. Zang R, Gomez Castro MF, McCune BT, Zeng Q, Rothlauf PW, Sonnek NM, Liu Z, Brulois KF, Wang X, Greenberg HB, Diamond MS, Ciorba MA, Whelan SPJ, Ding S. 2020. TMPRSS2 and TMPRSS4 promote SARS-CoV-2 infection of human small intestinal enterocytes. Sci Immunol 5.
3. Bojkova D, McGreig JE, McLaughlin K-M, Masterson SG, Widera M, Krähling V, Ciesek S, Wass MN, Michaelis M, Cinatl J. 2020. SARS-CoV-2 and SARS-CoV differ in their cell tropism and drug sensitivity profiles. bioRxiv 2020.04.03.024257.
4. Hui KPY, Cheung M-C, Perera RAPM, Ng K-C, Bui CHT, Ho JCW, Ng MMT, Kuok DIT, Shih KC, Tsao S-W, Poon LLM, Peiris M, Nicholls JM, Chan MCW. 2020. Tropism, replication competence, and innate immune responses of the coronavirus SARS-CoV-2 in human respiratory tract and conjunctiva: an analysis in ex-vivo and in-vitro cultures. Lancet Respir Med.
5. Li W, Moore MJ, Vasilieva N, Sui J, Wong SK, Berne MA, Somasundaran M, Sullivan JL, Luzuriaga K, Greenough TC, Choe H, Farzan M. 2003. Angiotensin-converting enzyme 2 is a functional receptor for the SARS coronavirus. Nature 426:450–454.
6. Letko M, Marzi A, Munster V. 2020. Functional assessment of cell entry and receptor usage for SARS-CoV-2 and other lineage B betacoronaviruses. Nat Microbiol 5:562–569.
7. Hoffmann M, Kleine-Weber H, Schroeder S, Krüger N, Herrler T, Erichsen S, Schiergens TS, Herrler G, Wu N-H, Nitsche A, Müller MA, Drosten C, Pöhlmann S. 2020. SARS-CoV-2 Cell Entry Depends on ACE2 and TMPRSS2 and Is Blocked by a Clinically Proven Protease Inhibitor. Cell.
8. Heald-Sargent T, Gallagher T. 2012. Ready, set, fuse! The coronavirus spike protein and acquisition of fusion competence. Viruses 4:557–580.
9. Matsuyama S, Nao N, Shirato K, Kawase M, Saito S, Takayama I, Nagata N, Sekizuka T, Katoh H, Kato F, Sakata M, Tahara M, Kutsuna S, Ohmagari N, Kuroda M, Suzuki T, Kageyama T, Takeda M. 2020. Enhanced isolation of SARS-CoV-2 by TMPRSS2-expressing cells. Proc Natl Acad Sci U S A 117:7001–7003.
10. Shulla A, Heald-Sargent T, Subramanya G, Zhao J, Perlman S, Gallagher T. 2011. A transmembrane serine protease is linked to the severe acute respiratory syndrome coronavirus receptor and activates virus entry. J Virol 85:873–882.
11. Ou X, Liu Y, Lei X, Li P, Mi D, Ren L, Guo L, Guo R, Chen T, Hu J, Xiang Z, Mu Z, Chen X, Chen J, Hu K, Jin Q, Wang J, Qian Z. 2020. Characterization of spike glycoprotein of SARS-CoV-2 on virus entry and its immune cross-reactivity with SARS-CoV. 1. Nat Commun 11:1–12.
12. Hoffmann M, Kleine-Weber H, Pöhlmann S. 2020. A Multibasic Cleavage Site in the

Spike Protein of SARS-CoV-2 Is Essential for Infection of Human Lung Cells. Mol Cell 78:779-784.e5.
13. Giacca M, Bussani R, Schneider E, Zentilin L, Collesi C, Ali H, Braga L, Secco I, Volpe MC, Colliva A, Zanconati F, Berlot G, Silvestri F, Zacchigna S. 2020. Persistence of viral RNA, widespread thrombosis and abnormal cellular syncytia are hallmarks of COVID-19 lung pathology. medRxiv 2020.06.22.20136358.
14. Ziegler CGK, Allon SJ, Nyquist SK, Mbano IM, Miao VN, Tzouanas CN, Cao Y, Yousif AS, Bals J, Hauser BM, Feldman J, Muus C, Wadsworth MH, Kazer SW, Hughes TK, Doran B, Gatter GJ, Vukovic M, Taliaferro F, Mead BE, Guo Z, Wang JP, Gras D, Plaisant M, Ansari M, Angelidis I, Adler H, Sucre JMS, Taylor CJ, Lin B, Waghray A, Mitsialis V, Dwyer DF, Buchheit KM, Boyce JA, Barrett NA, Laidlaw TM, Carroll SL, Colonna L, Tkachev V, Peterson CW, Yu A, Zheng HB, Gideon HP, Winchell CG, Lin PL, Bingle CD, Snapper SB, Kropski JA, Theis FJ, Schiller HB, Zaragosi L-E, Barbry P, Leslie A, Kiem H-P, Flynn JL, Fortune SM, Berger B, Finberg RW, Kean LS, Garber M, Schmidt AG, Lingwood D, Shalek AK, Ordovas-Montanes J, HCA Lung Biological Network. Electronic address: lung-network@humancellatlas.org, HCA Lung Biological Network. 2020. SARS-CoV-2 Receptor ACE2 Is an Interferon-Stimulated Gene in Human Airway Epithelial Cells and Is Detected in Specific Cell Subsets across Tissues. Cell 181:1016-1035.e19.
15. Lucas JM, Heinlein C, Kim T, Hernandez SA, Malik MS, True LD, Morrissey C, Corey E, Montgomery B, Mostaghel E, Clegg N, Coleman I, Brown CM, Schneider EL, Craik C, Simon J, Bedalov T, Nelson PS. 2014. The Androgen-Regulated Protease TMPRSS2 Activates aProteolytic Cascade Involving Components of the Tumor Microenvironment and Promotes Prostate Cancer Metastasis. Cancer Discov 4:1310–1325.
16. Wrapp D, Wang N, Corbett KS, Goldsmith JA, Hsieh C-L, Abiona O, Graham BS, McLellan JS. 2020. Cryo-EM structure of the 2019-nCoV spike in the prefusion conformation. Science 367:1260–1263.
17. Nimishakavi S, Raymond WW, Gruenert DC, Caughey GH. 2015. Divergent Inhibitor Susceptibility among Airway Lumen-Accessible Tryptic Proteases. PLOS ONE 10:e0141169.
18. Shrimp JH, Kales SC, Sanderson PE, Simeonov A, Shen M, Hall MD. 2020. An Enzymatic TMPRSS2 Assay for Assessment of Clinical Candidates and Discovery of Inhibitors as Potential Treatment of COVID-19. BioRxiv Prepr Serv Biol.
19. Kim IS, Jenni S, Stanifer ML, Roth E, Whelan SPJ, van Oijen AM, Harrison SC. 2017. Mechanism of membrane fusion induced by vesicular stomatitis virus G protein. Proc Natl Acad Sci U S A 114:E28–E36.
20. Hoffmann M, Wu Y-J, Gerber M, Berger-Rentsch M, Heimrich B, Schwemmle M, Zimmer G. 2010. Fusion-active glycoprotein G mediates the cytotoxicity of vesicular stomatitis virus M mutants lacking host shut-off activity. J Gen Virol 91:2782–2793.
21. Hoffmann D, Bayer W, Wildner O. 2007. Therapeutic immune response induced by intratumoral expression of the fusogenic membrane protein of vesicular stomatitis virus and cytokines encoded by adenoviral vectors. Int J Mol Med 20:673–681.
22. Buchrieser J, Dufloo J, Hubert M, Monel B, Planas D, Rajah MM, Planchais C, Porrot F, Guivel-Benhassine F, Werf SV der, Casartelli N, Mouquet H, Bruel T, Schwartz O. 2020. Syncytia formation by SARS-CoV-2 infected cells. bioRxiv 2020.07.14.202028.
23. Azouz NP, Klingler AM, Rothenberg ME. 2020. Alpha 1 Antitrypsin is an Inhibitor of the SARS-CoV2–Priming Protease TMPRSS2. bioRxiv 2020.05.04.077826.
24. Yamamoto M, Kiso M, Sakai-Tagawa Y, Iwatsuki-Horimoto K, Imai M, Takeda M, Kinoshita N, Ohmagari N, Gohda J, Semba K, Matsuda Z, Kawaguchi Y, Kawaoka Y, Inoue J. 2020. The anticoagulant nafamostat potently inhibits SARS-CoV-2 infection in vitro: an

existing drug with multiple possible therapeutic effects. bioRxiv 2020.04.22.054981.
25. Liu S, Selvaraj P, Lien CZ, Wu WW, Chou C-K, Wang TT. 2020. The PRRA insert at the S1/S2 site modulates cellular tropism of SARS-CoV-2 and ACE2 usage by the closely related Bat raTG13. bioRxiv 2020.07.20.213280.
26. Xia S, Lan Q, Su S, Wang X, Xu W, Liu Z, Zhu Y, Wang Q, Lu L, Jiang S. 2020. The role of furin cleavage site in SARS-CoV-2 spike protein-mediated membrane fusion in the presence or absence of trypsin. Signal Transduct Target Ther 5.
27. Jaimes JA, Millet JK, Whittaker GR. 2020. Proteolytic Cleavage of the SARS-CoV-2 Spike Protein and the Role of the Novel S1/S2 Site. iScience 23:101212.
28. Simmons G, Bertram S, Glowacka I, Steffen I, Chaipan C, Agudelo J, Lu K, Rennekamp AJ, Hofmann H, Bates P, Pöhlmann S. 2011. Different host cell proteases activate the SARS-coronavirus spike-protein for cell-cell and virus-cell fusion. Virology 413:265–274.
29. Shang J, Wan Y, Luo C, Ye G, Geng Q, Auerbach A, Li F. 2020. Cell entry mechanisms of SARS-CoV-2. Proc Natl Acad Sci U S A.
30. Kleine-Weber H, Elzayat MT, Hoffmann M, Pöhlmann S. 2018. Functional analysis of potential cleavage sites in the MERS-coronavirus spike protein. Sci Rep 8:16597.
31. Hoffmann M. SARS-CoV-2 Cell Entry Depends on ACE2 and TMPRSS2 and Is Blocked by a Clinically Proven Protease Inhibitor 19.
32. Hoffmann M, Müller MA, Drexler JF, Glende J, Erdt M, Gützkow T, Losemann C, Binger T, Deng H, Schwegmann-Weßels C, Esser K-H, Drosten C, Herrler G. 2013. Differential Sensitivity of Bat Cells to Infection by Enveloped RNA Viruses: Coronaviruses, Paramyxoviruses, Filoviruses, and Influenza Viruses. PLoS ONE 8:e72942.

FIGURE LEGENDS

Figure 1: SARS-CoV-2-S mediates robust fusion activity in the presence of ACE2 and TMPRSS2 on target cells which is dependent on the S2' cleavage site.
A Schematic illustration of the Coronavirus Spike protein showing the Signal Peptide (SP), the Receptor Domain (RBD), the Fusion Peptide (FP), the Transmembrane Domain (TM), the S1S2 cleavage site (S1/S2) and the S2 cleavage site (S2'), together with amino acid sequence alignments of the spike proteins of SARS-CoV-2, SARS-CoV and the SARS-2 cleavage site mutants analyzed in this study (not exactly drawn to scale).
B Cell-Cell Fusion-Assay: Effector cells (293T transfected with either empty vector or expression plasmids for the indicated spike variants and Vp16-Gal4 transactivator) were cocultured together with target cells (293T transfected with empty vector or ACE2/TMPRSS2 expression plasmids and Gal4-TurboGFP-Luc reporter plasmid). After 48h luciferase activity was measured. The data shows averaged relative luminescence units, error bars represent the standard deviations of one representative experiment performed in triplicates.
C Expression of proteins in effector and target cells was analyzed before co-culture. Due to better detectability the processed low molecular weight TMPRSS2 variant is shown. The expression of GAPDH served as loading control. One representative Western blot is shown.
D Representative GFP fluorescence microscopy images of ACE2 and TMPRSS2 expressing cells from the cell-cell fusion assay shown in **B**, (200 µm scale bar).

Figure 2: SARS-CoV-2-S-mediated cell-cell fusion depends on ACE2 receptor expression whereas SARS-CoV-spike mediated fusion depends on TMPRSS2 activity in 293T cells.

A Cell-Cell Fusion-Assay: Effector cells (293T transfected with either empty vector or expression plasmids for the indicated spike variants together with Vp16-Gal4 expression plasmid) were added to target cells (293T transfected with empty vector, expression plasmids for ACE2, TMPRSS2 alone or in combination and Gal4-TurboGFP-Luc reporter plasmid), which had been pre-incubated for 30 min with Bromhexine, Ambroxol or Camostat. After addition of effector cells, effector und target cells were cocultured in the presence of the respective inhibitors at 50µM. After 24h luciferase activity was measured. The data shows averaged relative luminescence units and the error bars represent the standard error of the mean of four independent experiments, each performed in triplicates. Statistical significance was determined by Two-Way ANOVA, p-values were corrected for multiple comparisons by Sidak's method method ($p>0.05$, ns; $p\leq0.05$, *; $p\leq0.01$, **; $p\leq0.001$, ***; $p\leq0.0001$, ****). For the comparison between inhibitor treatments, the three comparisons within each family were corrected for. The p-values for comparisons between different H2O (control) treated target cell populations were corrected for multiple comparison of each target cell and effector cell combination in the inhibitor group (in total possible 190 comparisons).
B Representative panel of GFP fluorescence microscopy images from H_2O incubated samples from the cell-cell Fusion-Assay shown in **A** (200 µm scale bar).
C The expression of proteins in non-treated target cells and effector cells after co-cultivation was analyzed by western blot from lysates harvested for determination of luciferase activity. The predominant, processed low molecular weight TMPRSS2 fragment is shown. The expression of GAPDH served as loading control. One representative Western blot is shown.

Figure 3: SARS-CoV-2-S-mediated cell-cell fusion is enhanced by Bromhexine.
Cell-Cell Fusion-Assay: Effector cells (293T cells transfected with either empty vector or the indicated glycoprotein expression plasmids and Gal4-Luc reporter plasmid) were cocultured with target cells (293T transfected with empty vector or ACE2 and TMPRSS2 expression plasmids and Vp16-Gal4 expression plasmid) that were pre-incubated for 30 min with Bromhexine or Ambroxol. After addition of effector cells, effector und target cells were cocultured with inhibitors at indicated concentrations, and luciferase activity of cell lysates was measured after 48h. Data shows averaged relative luminescence units of one experiment performed in triplicates, error bars represent the standard deviation.

Figure 4: TMPRSS2-dependent entry of lentiviral and rhabdoviral particles pseudotyped with SARS-CoV-2-S is not specifically inhibited by Bromhexine or Ambroxol.
A, B 293T cells transfected with empty vector, ACE2/TMPRSS2, ACE2 or TMPRSS2 were pre-incubated with Bromehexine, Ambroxol or Camostat at indicated concentration before addition of Lentiviral particles pseudotyped with SARS-CoV-2-Spike (**A**) or VSV-G (**B**). 48h after transduction the cells were analysed via flow-cytometry. Data shows averaged percent of GFP-positive cells, error bars represent the standard deviations of one representative experiment performed in triplicates**. C** Images of ACE2 and TMPRSS2 transfected cells that were infected with the respective lentiviral pseudotype particles.
D Western Blot analysis of transfected 293T cells used for transduction-experiments in **A** and **B**. The predominant, processed, low molecular weight TMPRSS2 fragment is shown here. The expression of GAPDH served as loading control.

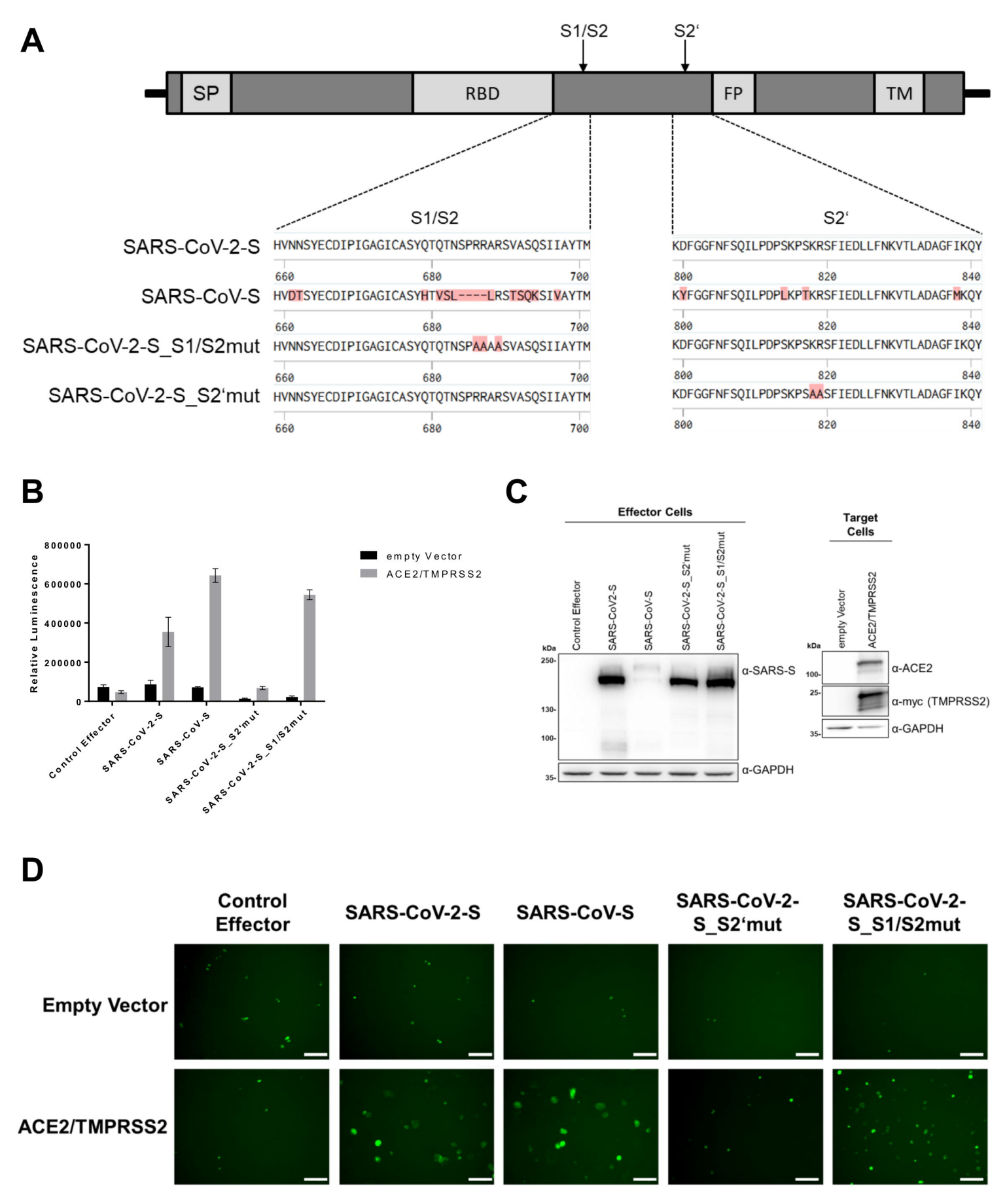
A
S1/S2
S2‘
SP
RBD
FP
TM
S1/S2
S2‘
SARS-CoV-2-S
HVNNSYECDIPIGAGICASYQTQTNSPRRARSVASQSIIAYTM
KDFGGFNFSQILPDPSKPSKRSFIEDLLFNKVTLADAGFIKQY
660 680 700
800 820 840
SARS-CoV-S
HVDTSYECDIPIGAGICASYHTVSL----LRSTSQKSIVAYTM
KYFGGFNFSQILPDPLKPTKRSFIEDLLFNKVTLADAGFMKQY
660 680 700
800 820 840
SARS-CoV-2-S_S1/S2mut
HVNNSYECDIPIGAGICASYQTQTNSPAAAASVASQSIIAYTM
KDFGGFNFSQILPDPSKPSKRSFIEDLLFNKVTLADAGFIKQY
660 680 700
800 820 840
SARS-CoV-2-S_S2‘mut
HVNNSYECDIPIGAGICASYQTQTNSPRRARSVASQSIIAYTM
KDFGGFNFSQILPDPSKPSAASFIEDLLFNKVTLADAGFIKQY
660 680 700
800 820 840
B
Relative Luminescence
800000
600000
400000
200000
0
empty Vector
ACE2/TMPRSS2
Control Effector
SARS-CoV-2-S
SARS-CoV-S
SARS-CoV-2-S_S2'mut
SARS-CoV-2-S_S1/S2mut
C
Effector Cells
Control Effector
SARS-CoV2-S
SARS-CoV-S
SARS-CoV-2-S_S2'mut
SARS-CoV-2-S_S1/S2mut
kDa
250-
130-
100-
35-
α-SARS-S
α-GAPDH
Target Cells
empty Vector
ACE2/TMPRSS2
kDa
100-
25-
35-
α-ACE2
α-myc (TMPRSS2)
α-GAPDH
D
Control Effector
SARS-CoV-2-S
SARS-CoV-S
SARS-CoV-2-S_S2‘mut
SARS-CoV-2-S_S1/S2mut
Empty Vector
ACE2/TMPRSS2

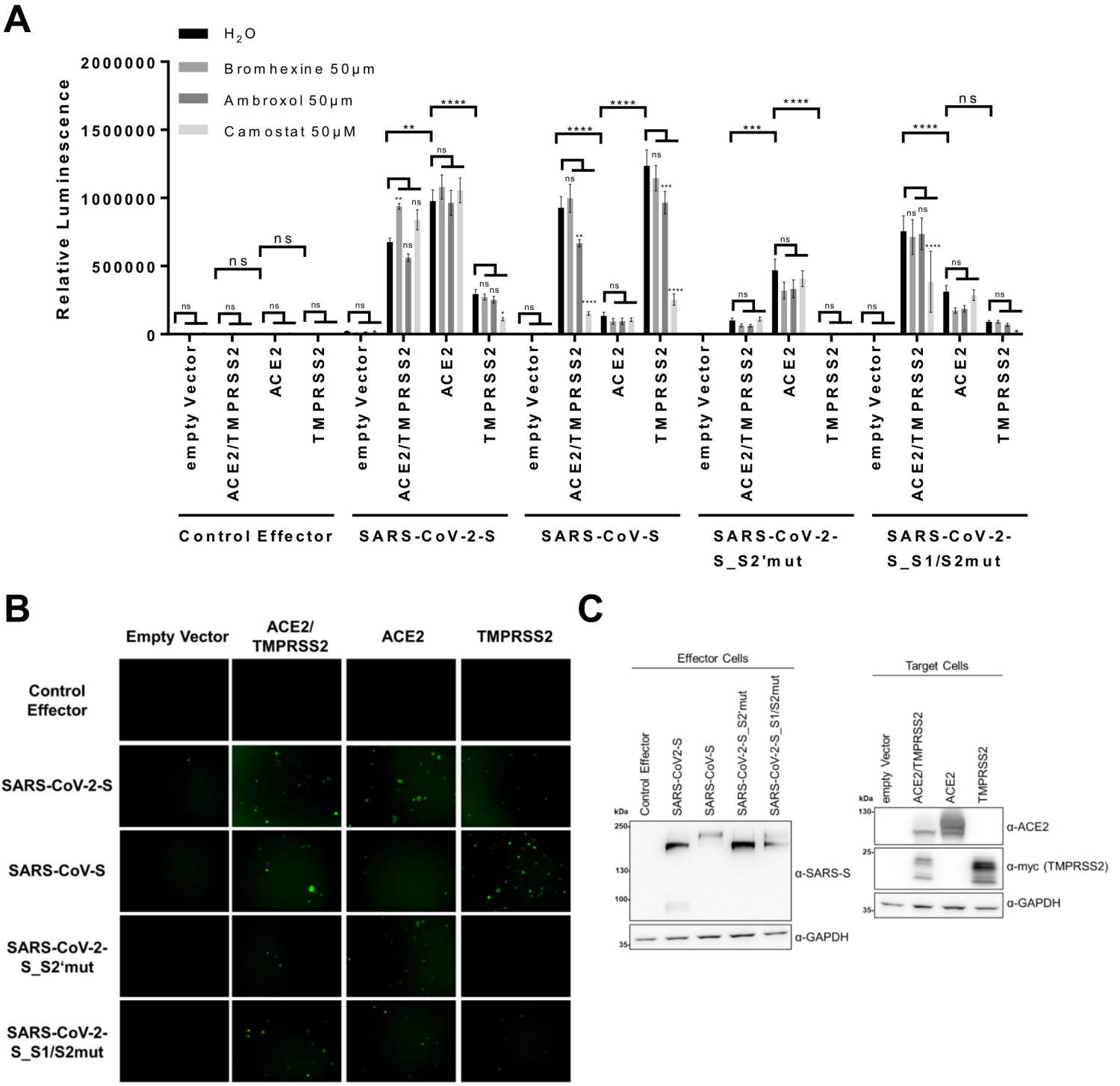
A
H2O
Bromhexine 50µm
Ambroxol 50µm
Camostat 50µM
Relative Luminescence
2000000
1500000
1000000
500000
0
empty Vector
ACE2/TMPRSS2
ACE2
TMPRSS2
Control Effector
SARS-CoV-2-S
SARS-CoV-S
SARS-CoV-2-S_S2'mut
SARS-CoV-2-S_S1/S2mut
B
Empty Vector
ACE2/ TMPRSS2
ACE2
TMPRSS2
Control Effector
SARS-CoV-2-S
SARS-CoV-S
SARS-CoV-2-S_S2'mut
SARS-CoV-2-S_S1/S2mut
C
Effector Cells
Control Effector
SARS-CoV2-S
SARS-CoV-S
SARS-CoV-2-S_S2'mut
SARS-CoV-2-S_S1/S2mut
kDa
250
130
100
35
α-SARS-S
α-GAPDH
Target Cells
empty Vector
ACE2/TMPRSS2
ACE2
TMPRSS2
130
25
35
α-ACE2
α-myc (TMPRSS2)
α-GAPDH

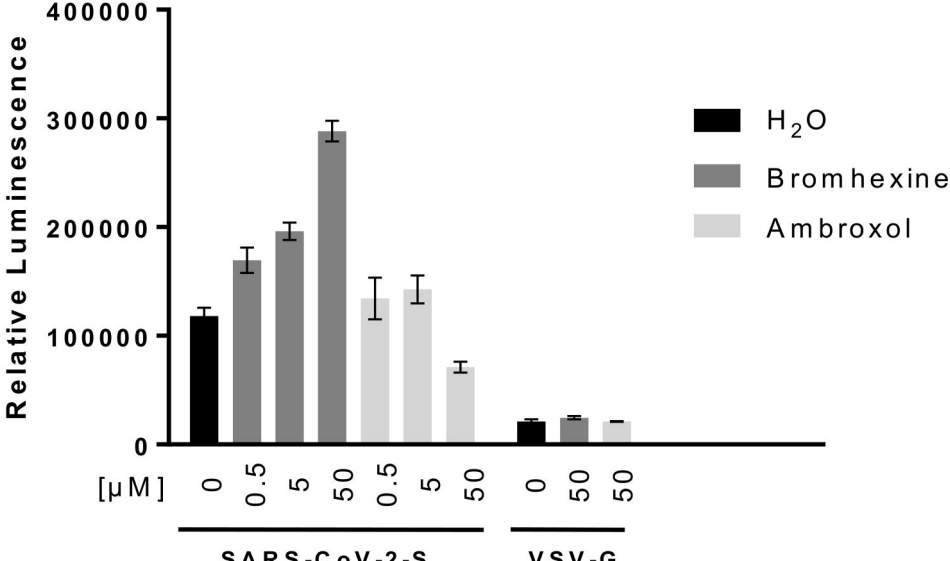
Relative Luminescence
400000
300000
200000
100000
0
H2O
Bromhexine
Ambroxol
[µM]
0
0.5
5
50
0.5
5
50
0
50
50
SARS-CoV-2-S
VSV-G

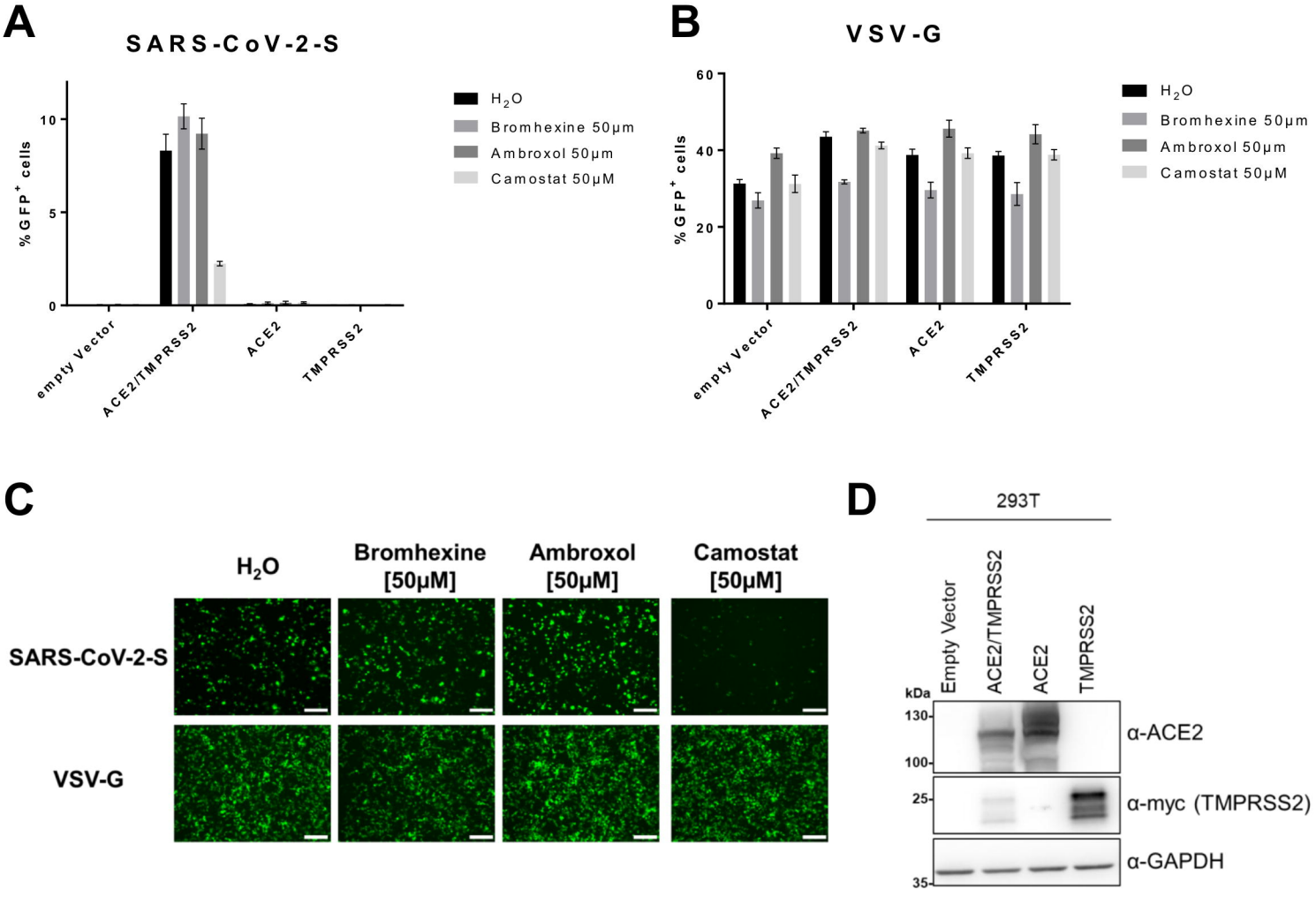
A
SARS-CoV-2-S
% GFP+ cells
10
5
0
empty Vector
ACE2/TMPRSS2
ACE2
TMPRSS2
H2O
Bromhexine 50µm
Ambroxol 50µm
Camostat 50µM
B
VSV-G
% GFP+ cells
60
40
20
0
empty Vector
ACE2/TMPRSS2
ACE2
TMPRSS2
H2O
Bromhexine 50µm
Ambroxol 50µm
Camostat 50µM
C
H2O
Bromhexine [50µM]
Ambroxol [50µM]
Camostat [50µM]
SARS-CoV-2-S
VSV-G
D
293T
Empty Vector
ACE2/TMPRSS2
ACE2
TMPRSS2
kDa
130
100
25
35
α-ACE2
α-myc (TMPRSS2)
α-GAPDH